Improving Electrical Power Quality During Photovoltaic Feed-in to the Power Distribution Grid Using a Parallel Active Filter with MPPT (P&O) Control

Abstract

This article identifies power quality issues related to the injection of solar photovoltaic power into the electrical distribution grid and proposes solutions aimed at improving consumers' energy efficiency. Various configurations are studied and simulated using MATLAB/Simulink. The study focuses on disturbances in voltage and current waveforms, the harmonic distortion ratio (evaluated according to the IEEE 519-1996 standard), and the reactive power absorbed by nonlinear loads. The final configuration connects a photovoltaic generator to the grid via a parallel active filter with an LC structure, a BOOST chopper controlled by an MPPT using the P&O method, and a power converter. Simulations of this configuration yield generally satisfactory results, with a total harmonic distortion (THD) of 0.49%, in compliance with the IEEE 519-1996 standard.

Key words: Power quality, photovoltaic solar energy, parallel active filter, total harmonic distortion (THD), MPPT (P&O), IEEE 519-1996.

1. Introduction

Fossil fuels such as coal, oil, natural gas, etc., are considered finite and polluting resources but are essential for the production of electrical energy **[1–3]**. Given the world's growing energy needs, does the exploitation of these energy sources not pose a major environmental threat to the future of our planet? By referring to international treaties on climate issues, such as the Kyoto Protocol (December 1997), the Durban Conference (September 2001), the Bali Plan (December 2007), and the Cancun Agreement (December 2010) serve as warnings to prioritize green energy over fossil fuels **[4–7]**.

The energy crisis of recent years has prompted researchers around the world to focus on renewable energy as an alternative **[8–10]**. In this context, several countries have committed

UNDER PEER REVIEW IJAR

to harnessing these sources to partially replace conventional energy sources. It should be noted that there are several sources of renewable energy, including: water, wind, solar, biomass, geothermal, etc**[11–13]**. The energy transition requires the interconnection of the existing power grid with renewable energy sources **[14–16]**. Certain interconnections, such as photovoltaic systems, tend to degrade the grid, leading to power quality issues. The main objective of this article is to identify problems related to power quality on the electrical grid when photovoltaic solar energy is fed into the distribution grid and to propose improvements that enhance energy efficiency for consumers.

Currently, researchers have proposed several solutions for improving power quality, derived from simulations **[17–19]**. A key finding from this research is that filters generally offer a good compromise for improving power quality **[20–22]**. In the remainder of this article, we propose the use of an active filter in parallel with the MPPT controller, combined with the P&O method, to provide the best power quality to consumers and avoid unnecessary decoupling of the renewable source.

This article is structured into three sections. The first section provides an introduction to this article. The second section presents an evaluation of the performance and reliability of our proposed system using MATLAB/Simulink, taking into account variations in irradiance and temperature. Finally, the conclusion is presented in the third section.

2. Results

In this article, we use the parallel active filter shown in Figure 1 to clean up the power grid in order to compensate for harmonic current disturbances and improve power quality.

UNDER PEER REVIEW IJAR

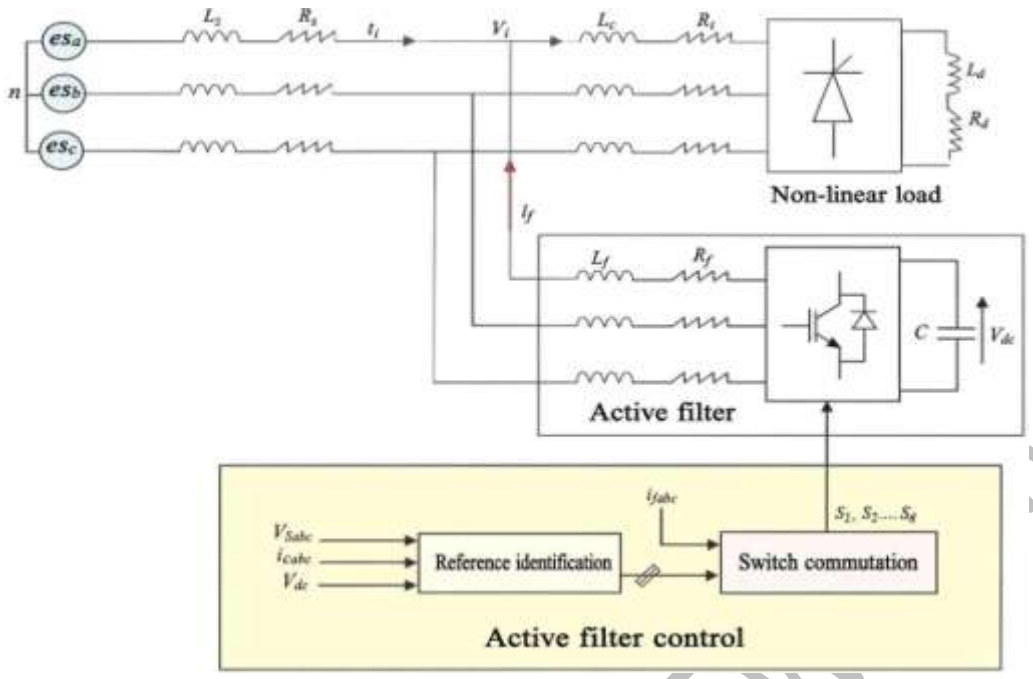


Figure 1: Parallel active filter structure.

The parallel active filter shown in Figure 1 is a shunt compensator because it consists of a harmonic current source generated by nonlinear loads and addresses both the power factor and reactive power issues. The configuration is such that the inverter is connected in parallel with the grid via a coupling element (passive filter) and an energy storage source. Figure 2 shows the overall system and the parallel active filter.

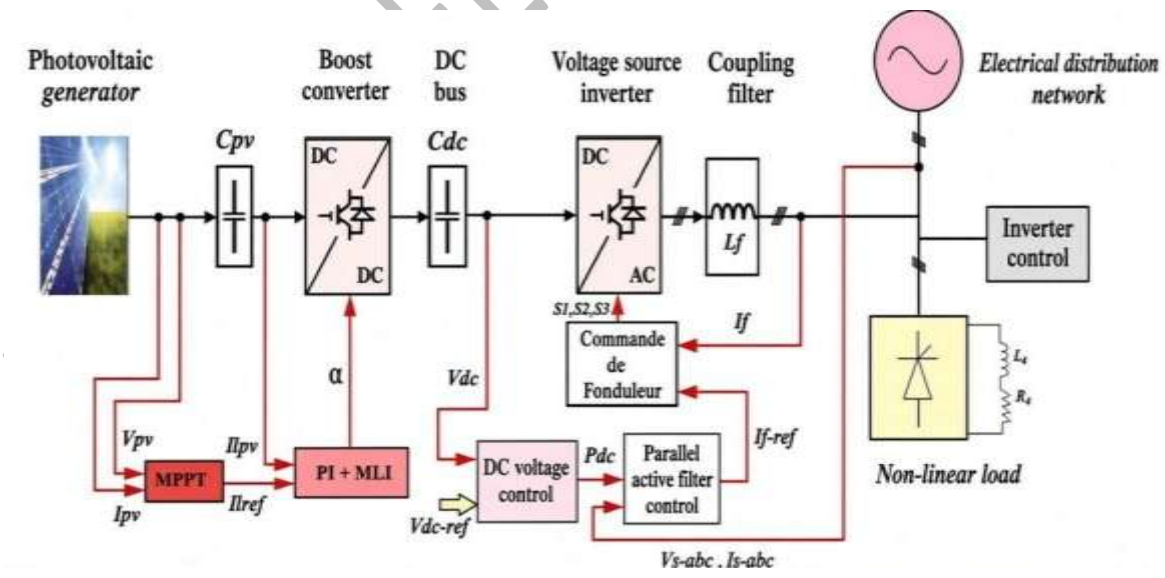


Figure 2: Proposed overall structure of the entire system.

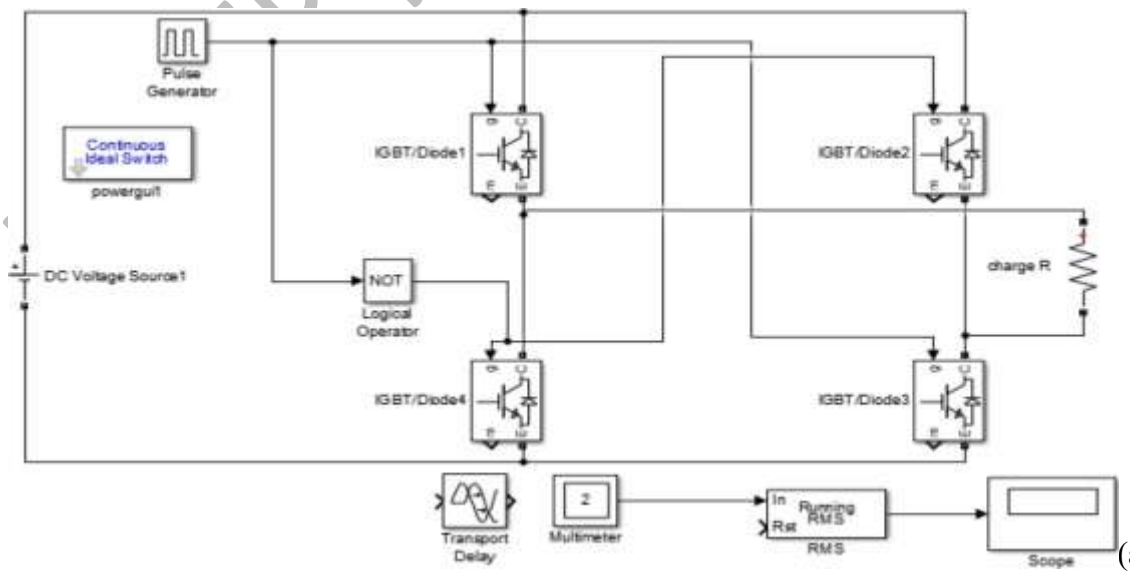
The entire system shown in Figure 2 consists of a photovoltaic generator, a power conversion unit, a coupling filter between the grid and the photovoltaic inverter, and a voltage inverter.

UNDER PEER REVIEW

The voltage inverter is the main actuator in this system, which incorporates a parallel active filter to provide all the necessary functionality and contribute to system services, such as reactive power compensation, current harmonic mitigation, and grid voltage balancing. For each configuration shown in Figure 2, a performance analysis and evaluation are conducted to validate the system's performance. Simulations of the overall system under study (photovoltaic generator with a BOOST inverter, the voltage inverter, parallel active filter, and nonlinear loads connected to a MV power grid) are performed in the MATLAB/Simulink environment, with the objective of obtaining an unbiased and concrete analysis of the simulation results and characterizing the behavior of the system under study. The load used in this simulation is a three-phase PD3 diode rectifier bridge connected to a resistive load (Rd), and the power grid is modeled by a perfectly sinusoidal three-phase voltage source in series with internal impedances (Rs, Ls). The SUNPOWER SPR-305 WHT-D photovoltaic generator, with a current of 5.4 A and a Vco voltage of 64.2 V, consists of 71 modules connected in series and 260 modules connected in parallel.

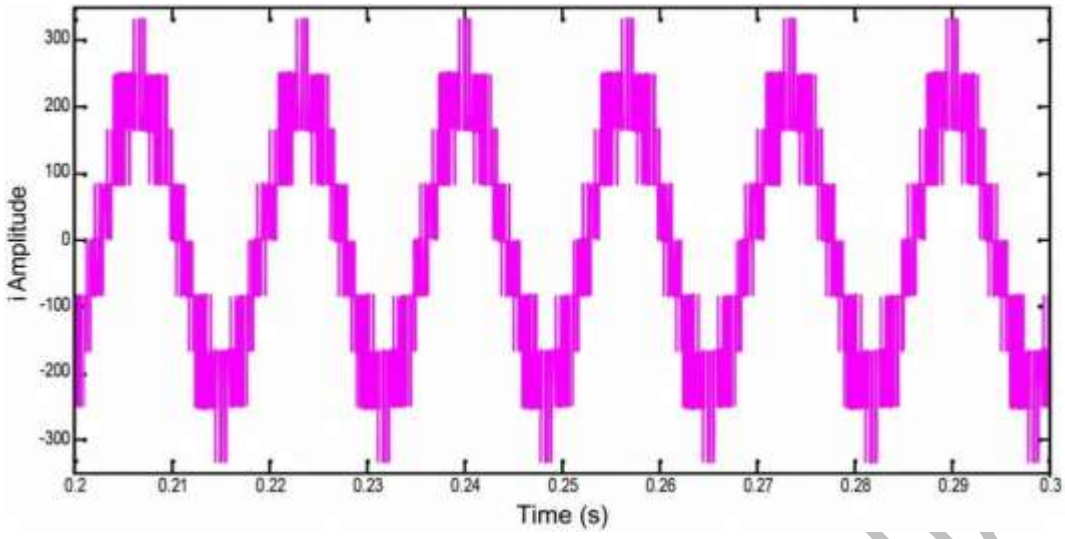
2.1 Results of Simulations for DC-Source and AC-Source Networks

In this article, we aimed to take a step-by-step approach by simulating a simple power system to observe the harmonic distortion ratio, then comparing this ratio when a nonlinear load was connected to the system, and finally interfacing the system and load via a parallel active filter. Figure 3 shows the power system with a DC source and the simple voltage signal from the inverter.



(a)

UNDER PEER REVIEW IJAR



(b)

Figure 3: (a) Electrical network with a DC source and (b) the inverter's simple voltage signal.

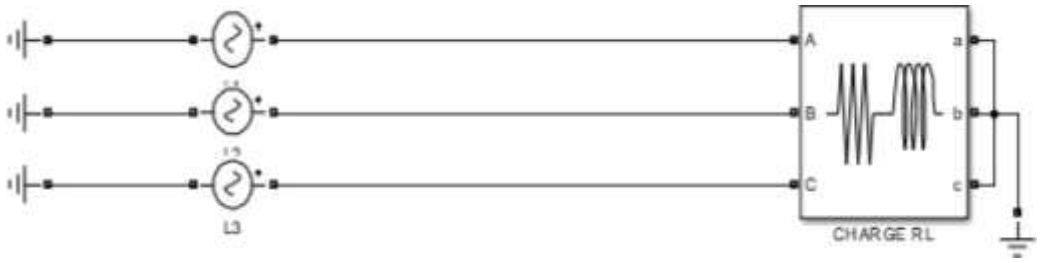
Figure 3 (a) consists of a 400 V DC source supplying a 100 Ω resistor, across which a converter (single-phase inverter) is connected. Figure 3 (b) shows the waveform of the voltage as a jagged and noisy waveform, far from being sinusoidal; this indicates that the inverter itself contains undesirable harmonics that affect the proper operation of the power system. This is assessed asa harmonic distortion rate of 11.49%, which does not comply with the international standard IEEE 519-1996, which requires a harmonic distortion rate of ≤ 5%. To study the behavior of the voltage from the AC grid and the current signal of the linear load. The parameters in Table 1 are used during the simulations.

Table 1: Simulation parameters for the single-phase power grid.

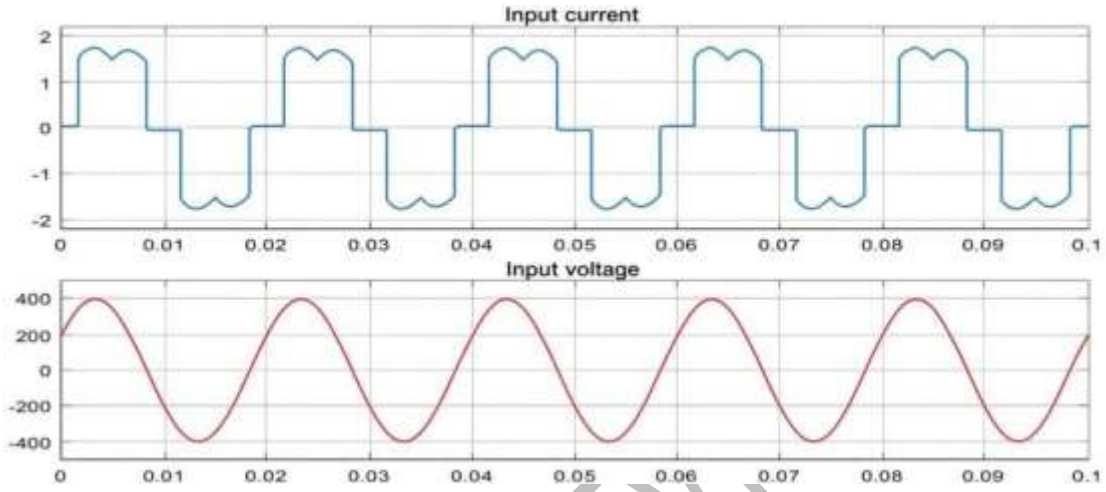
SystemComponent	Parameters	Values
Single-phaseelectricalgrid	Voltage	V=230,2[redacted]
	Frequency	f= 50 Hz
	Internalresistance	R_s= 3.5mΩ
	Internalinductance	L_s=5 nH

Figure 4 shows the AC power network, the voltage signal, and the current signal of the network before it is connected to the nonlinear load.

UNDER PEER REVIEW IJ...



(a)



(b)

Figure 4: (a) AC power network and (b) voltage and current signals of the network before being connected to the nonlinear load.

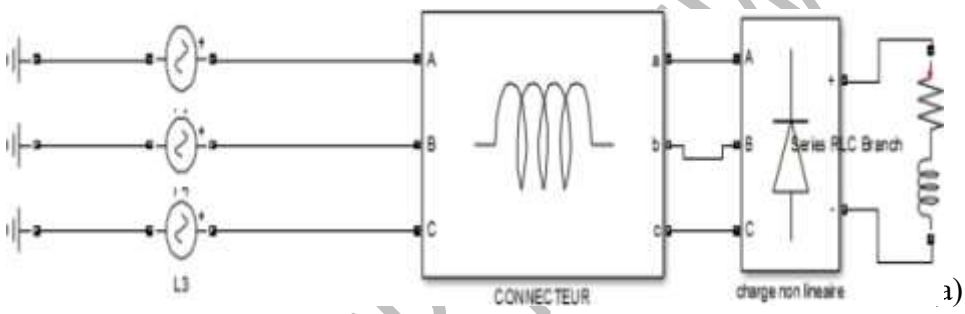
Figure 4 shows the waveforms of the grid voltage and current signals, which are in phase. The current waveform shows a zero-crossing point, and a small notch is also observed on the same current waveform. This noise originates from the grid itself and degrades the power quality delivered to consumers. It should be noted that the connected load is of even order. In contrast, the voltage waveform is clearly sinusoidal. The harmonics from the grid and the nonlinear load will be extracted in the preceding step. In Figure 4(a), a nonlinear load consisting of a PD3 bridge and a resistive inductor is added, from which the harmonic distortion rates are extracted. The parameters in Table 2 are used for the simulations of the configuration shown in Figure 5(a).

Table 2: Parameters of the electrical network with a nonlinear load.

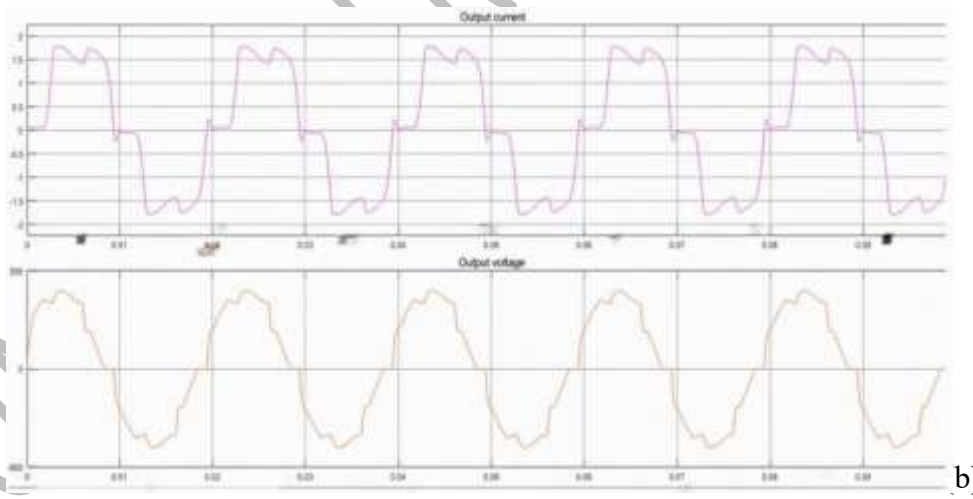
System components	Parameters	Values
Power system	Voltage	$V = 230, \sqrt{2}$ V

UNDER PEER REV.

	Frequency	f = 50 Hz
	Internalresistance	R_s= 3.5mΩ
	Internal inductance	L_s = 50nH
Nonlinearload	Filter impedance at the input of the PD3 bridge	L_d = 0.82mH
		R_c= 0.82mΩ
		L_c = 0.023mH



a)



b)

Figure 5: (a) Three-phase network connected to the nonlinear load and (b) voltage and current signals of the nonlinear load before the parallel active filter.

The voltage and current signals in Figure 5(b) are distorted. These harmonics result from the currents drawn by the nonlinear loads (rectifier + R-L load), which are superimposed on

theharmonics generated by the sinusoidal source. The harmonics of the load before the parallel active filter are shown in Figure 6.

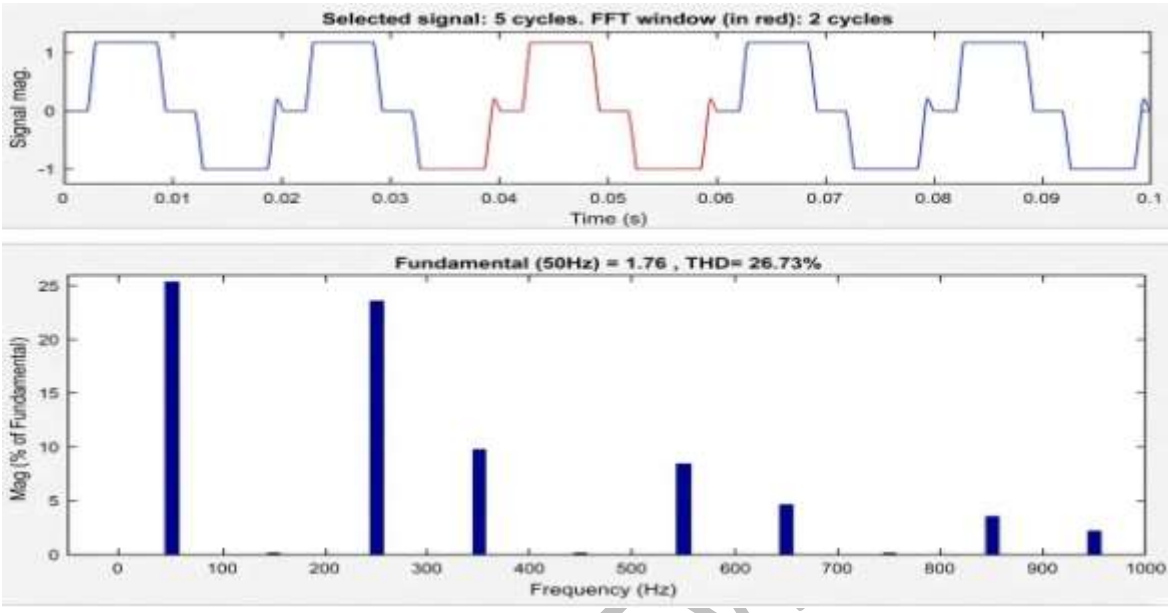


Figure 6: Load harmonics before the parallel active filter.

The harmonic distortion rate obtained from Figure 5 (a) is 26.73%, which is more than five times the international standard required by IEEE 519-1996. Since this parameter must be ≤ 5%, this is what truly accounts for the degradation in the quality of the power supplied to the loads. To improve power quality for consumers and prevent grid pollution caused by the nonlinear loads connected to it, it is advisable to install a parallel active filter in order to meet the requirements of the international standard regarding the harmonic distortion rate. The simulation parameters are shown in Table 3.

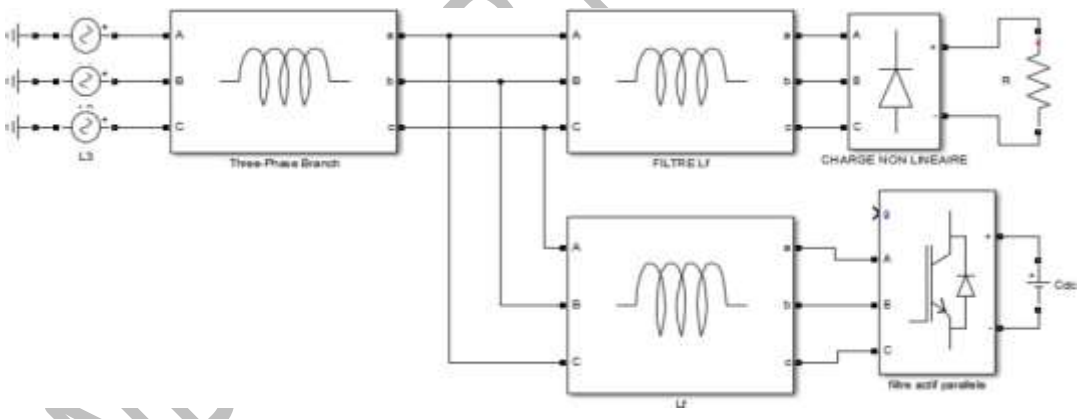
Table 3: Simulation parameters with a parallel active filter.

System component	**Parameters**	**Values**
Power grid	Voltage	$V = 230\sqrt{2}$ V
	Frequency	f = 50 Hz
	Internal resistance	R_s= 3.5 mΩ

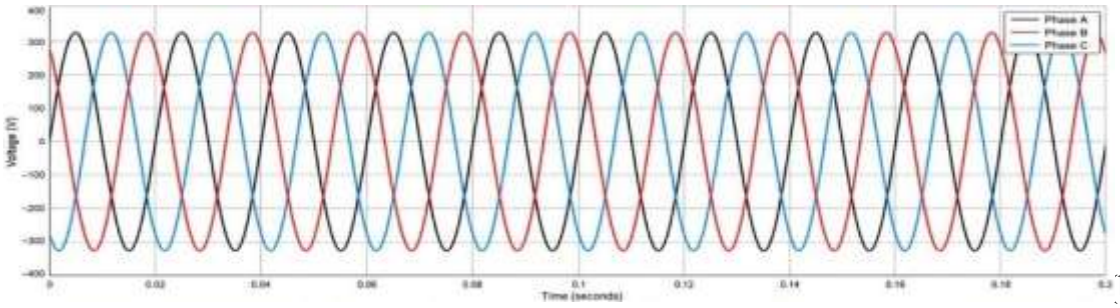
UNDER PEER REVIEW

	Internal inductance	L_s = 50 nH
Nonlinear Load	Rectifier bridge	R_d = 301
	Three-phase (PD3) power supply	L_d = 0.82 mH
		R_c= 0.82 mΩ
		L_c = 0.023 mH
Parallel active filter	Storage Capacitor	C_{dc}= 5.87 mF
	Output filter	L_f = 145 µH
	DC bus Voltage	V_{dc}= 850 V

Figure 7 shows the circuit topology used for the network and filter simulation, as well as the three-phase voltage and current after the parallel active filter.

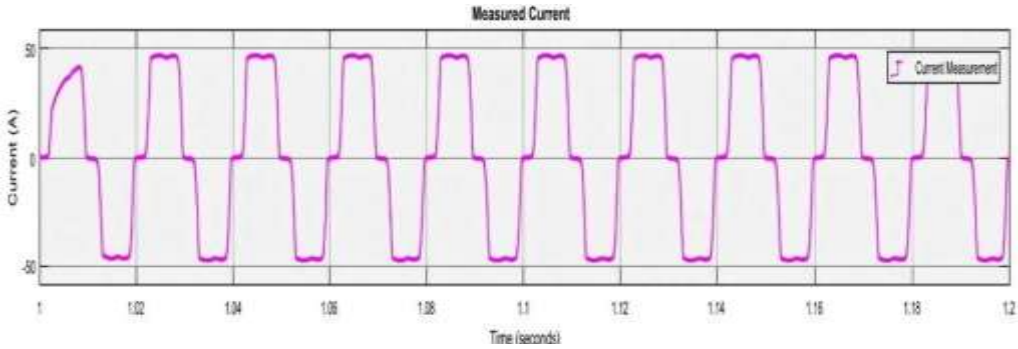


(a)



(b)

UNDER PEER REVIEW IJAR



c)

Figure 7: (a) Structure implemented for the network and filter simulation, (b) three-phase voltage signal after the filter, and (c) current signal after the parallel active filter.

The results shown in Figures 7(b) and (c) are satisfactory after the parallel active filter was added to the system. An improvement in the waveforms of the voltage and load current curves can be observed. The load harmonics after the parallel active filter are shown in Figure 8.

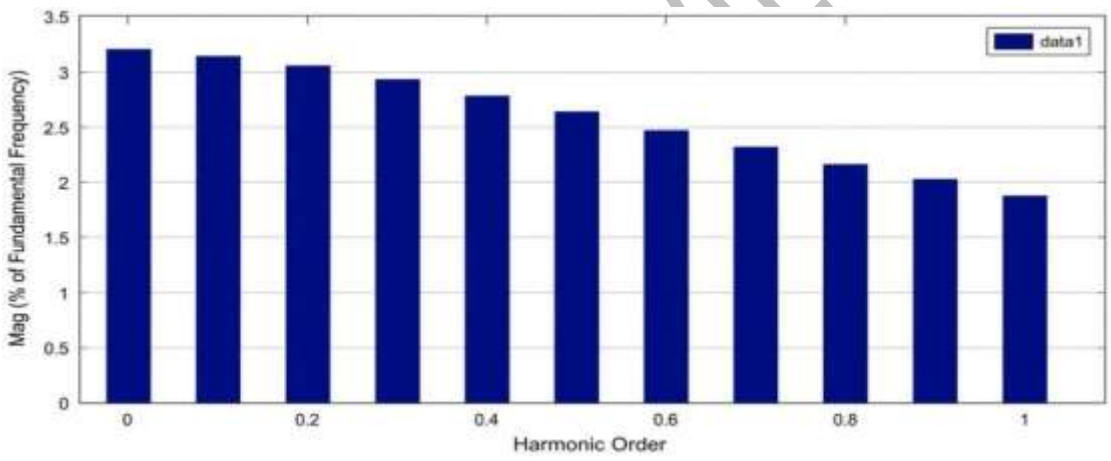


Figure 8: Harmonics after the parallel active filter.

In Figure 8, the performance of the parallel active filter reduced the harmonic distortion rate by 98%. Thus, the harmonic distortion rate is 1.94%, which complies with the standard published by the International Electro-technical Commission (IEC) IEEE 519-1996, as the value is less than 5% (harmonic distortion rate ≤ 5%).

2.2Simulation Results for the Grid-Connected Solar System

The system under study consists of PV panels, a BOOST chopper coupled with an MPPT and controlled by the P&O method, and an inverter interfaced with the parallel active filter, through which this solar energy is fed into the medium-voltage (MV) power grid in the

UNDER PEER REVIEW IJAR

MATLAB/Simulink environment under standard conditions of temperature T = 25°C and irradiance of1000 W/$m2$ of the entire system. The simulation of the system shown in Figure 9 does not include the parallel active filter.

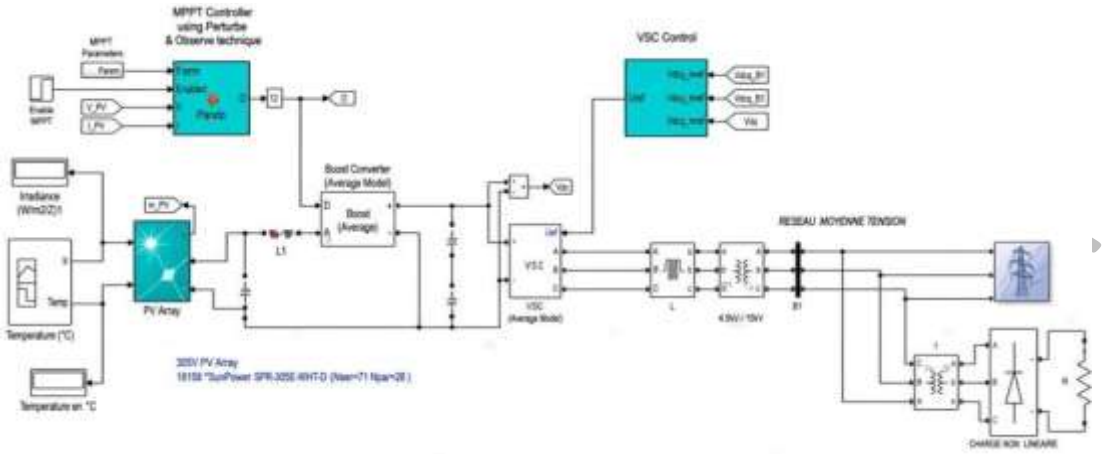


Figure 9: Simulated system before the parallel active filter.

The system shown in Figure 9 consists of a photovoltaic generator with a BOOST chopper and an inverter connected to the MV grid. The simulated parameters are listed in Table 4.

Table 4: Characteristics of the photovoltaic panels.

SystemComponent	Parameters	Values
Photovoltaicgenerator	Standard irradiance	G= 1000W/m^2
	Standardtemperature	T= 25°C
	Cellsinseries	N_s= 71
	Cellsinparallel	N_p= 260
	Maximumpower	P= 305.24 Wp
	Open-circuit voltage	V_{OC}= 64.2 V
	Short-circuitcurrent	I_{CC}=5.9A

The goal is always to observe the behavior of the voltage, current, and reactive power flow signals, as shown in Figure 10.

UNDER PEER REVIEW

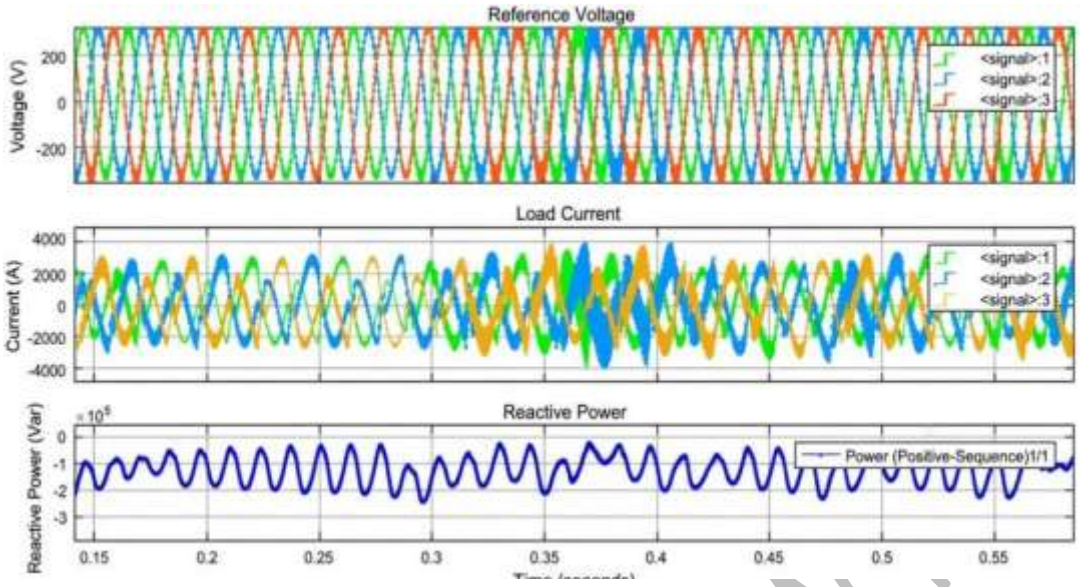


Figure 10: Voltage, current, and power signals without a parallel active filter.

The results in Figure 10 show a balanced reference voltage ($V_{dc\text{-}ref}$ = 380 V) with a well-defined sinusoidal waveform. We can conclude that the nonlinear load and the conversion equipment have no direct influence on the voltage waveform due to the MPPT control. However, the current waveforms are distorted, and the sinusoidal shapes are noisy. This is due to harmonics injected into the grid by the nonlinear loads and power conversion equipment. This noise observed in the current signals indicates a degradation in the power quality of the electrical grid. It can thus be observed that the reactive power fluctuates and enters the negative region. This leads to phase shift and power factor issues. Nonlinear loads place a higher demand on reactive power.

To observe the actual performance of the parallel active filter within the entire system, the system shown in Figure 11 is simulated using the parameters in Table 5.

Table 5: Panel specifications.

Different parts of the system	Parameters	Values
Photovoltaic generator	Standard solar radiation	G = 1000 W/m^2
	Standard temperature	T = 25°C
	Cells in series	N_s = 71

UNDER PEER REVIEW

	Cells in parallel	$N_p = 260$
	Maximum power	P = 305,24 Wc
	Open-circuit voltage	V_{CO} = 64.2 A
	Open-circuit current	I_{CO} = 5.9 A
Electric grid	Power grid frequency	f = 50 Hz
	Medium-voltage	V = 15 kV
	Apparent power	S = 30 kVA
Parallel active filter	Coupling inductance	L_f = 5.976 µH
	Storage capacitor	C = 198.94 µF

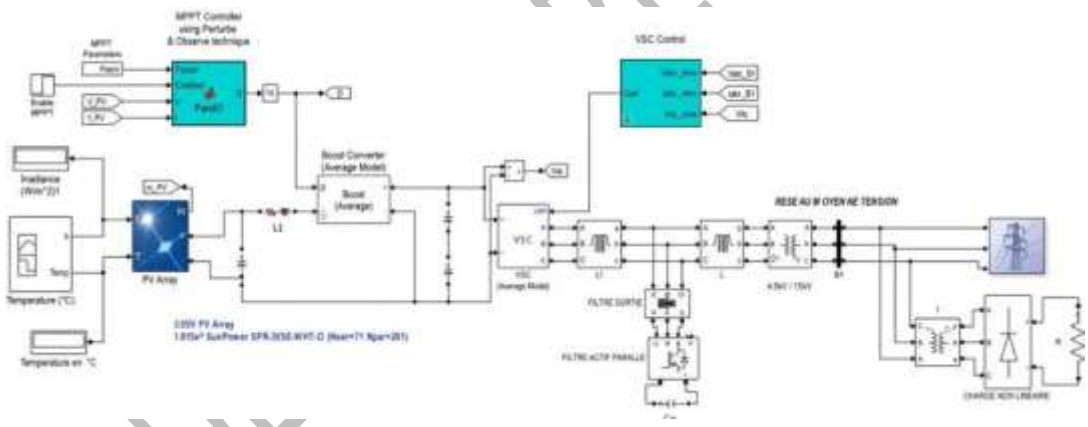


Figure 11: Schematic of the entire system with the parallel active filter.

The entire system shown in Figure 11 consists of a photovoltaic generator with a BOOST chopper and an inverter connected to the MV grid via a parallel active filter. The voltage, current, and power signals after the filter are shown in Figure 12.

UNDER PEER REVIEW IJAR

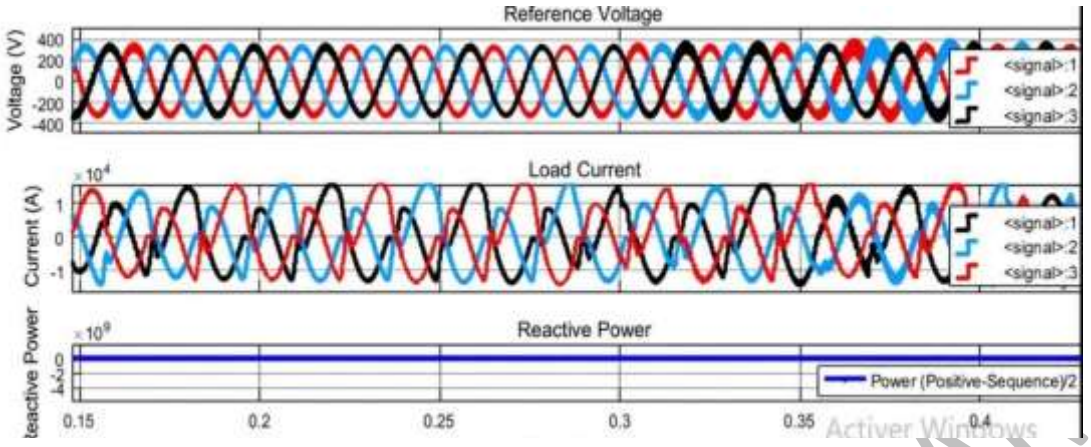


Figure 12: Voltage, current, and power signals after the parallel active filter.

After the active filter connected in parallel with the overall system (GPV, BOOST Inverter, inverter, active filter, and the grid), Figure 12 shows the expected result. The reference voltage remains balanced at all times, and the sinusoidal waveform is maintained and perfectly tracks its reference value ($V_{dc\text{-}ref}$ = 380 V) thanks to the robustness of the MPPT control. The noise observed in the current signals before the parallel active filter was filtered out following the injection of compensation current into the grid by the parallel active filter, which allowed the grid current signals to become smooth and sinusoidal, thereby ensuring good power quality for the electrical grid. It should be noted that the current zero-crossings in these signals occur at negligible intervals and do not cause any disturbances to power quality. On the same graph, at the far right, the curve shows the reactive power Q (var), which is zero. This is because the parallel active filter compensated for the reactive energy consumed by the nonlinear loads, which would have fluctuated in the absence of the parallel active filter. The harmonics of the entire system are shown in Figure 13.

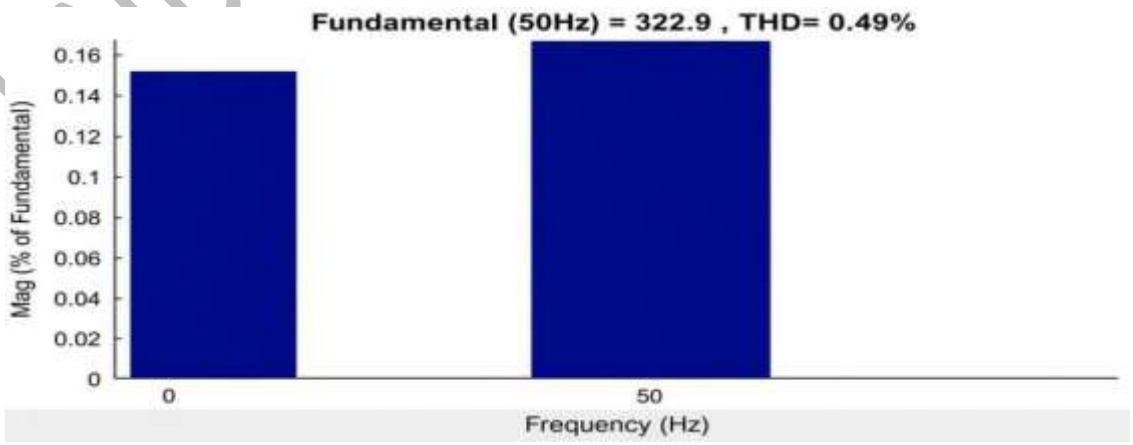


Figure 13: Harmonics of the entire system.

UNDER PEER REVIEW UAF

As shown in Figure 13, the objective of this article is also to reduce the harmonic distortion rate to a value less than or equal to 5% (harmonic distortion rate ≤ 5%) in accordance with the requirements of the International Electro-technical Commission's international standard. Consequently, the simulation results shown in Figure 13 indicate a harmonic distortion rate of 0.49%, which complies with the IEEE 519-1996 international standard.

3. Conclusion

The increase in electrical productivity resulting from feeding solar photovoltaic energy into the power grid used as a solution to provide access to energy services has negative effects on the grid's proper operation. For this reason, the objective of this article is to propose effective and tangible solutions to either reduce or completely eliminate these impacts in order to provide high-quality energy and meet users' needs. This article has identified problems caused by the injection of photovoltaic energy into the power grid. We focused particularly on the issue of grid power quality, which is disrupted by harmonics whether due to phase imbalance or excessive reactive power generation. This problem was solved by implementing a system that combines a photovoltaic generator, a BOOST-type inverter with MPPT control, an inverter to convert the energy from the photovoltaic generator, and a parallel active filter that filters the energy and injects harmonic current into the grid for compensation, which was then fed into the power grid. Simulations were performed using Matlab/Simulink software under standard metrological conditions of irradiance and temperature. The results obtained were satisfactory.Thus, we achieved the objective of this article, which was to reduce harmonics while clearly complying with the international standard of the International Electro-technical Commission and to transfer all the energy produced by the photovoltaic generator to the power grid in order to improve power quality and simultaneously compensate for the reactive power drawn by the load. Compared to the results examined in various studies cited in this article, it was noted that the result obtained in terms of the harmonic distortion ratio is better.

3.References

UNDER PEER REVIEW IJAR

252 **[1]**Kabeyi, M.J.B. and Olanrewaju, O.A., Sustainable energy transition for renewable and
253 low-carbon grid electricity generation and supply, Frontiers in Energy Research, 9,
254 743114 (2022).
255 **[2]** Balat, M.M.Y.C., "Status of fossil energy resources: A global perspective. Energy
256 Sources, Part B: Economics, Planning, and Policy, 2(1), 31–47 (2007).
257 **[3]**Arutyunov, V.S. and Lisichkin, G.V., Energy resources of the 21st century: problems and
258 forecasts. Can renewable energy sources replace fossil fuels?, Russian Chemical
259 Reviews 86(8), 777–804 (2017).
260 **[4]**Breidenich, C., Magraw, D., Rowley, A., and Rubin, J.W., The Kyoto Protocol to the
261 United Nations Framework Convention on Climate Change, American Journal of
262 International Law 92(2), 315–331 (1998).
263 **[5]**Deleuil, T., The common but differentiated responsibilities principle: Changes in
264 continuity after the Durban Conference of the Parties, Review of European
265 Community & International Environmental Law 21(3), 271–281 (2012).
266 **[6]**Ott, H.E., Sterk, W., and Watanabe, R., The Bali Roadmap: New Horizons for Global
267 Climate Policy, Climate Policy, 8(1), pp. 91–95 (2008).
268 **[7]**Truxal, S., The ICAO Assembly Resolutions on International Aviation and Climate
269 Change: An Historic Agreement, a Breakthrough Deal, and the Cancun Effect, Air and
270 Space Law, 36(3) (2011).
271 **[8]**Farghali, M., Osman, A.I., Mohamed, I.M., Chen, Z., Chen, L., Ihara, I., Yap, P.S., and
272 Rooney, D.W., Strategies to Save Energy in the Context of the Energy Crisis: A
273 Review, Environmental Chemistry Letters 21(4), 2003–2039 (2023).
274 **[9]**Gajdzik, B., Wolniak, R., Nagaj, R., Žuromskaitė-Nagaj, B., and Grebski, W.W., The
275 influence of the global energy crisis on energy efficiency: A comprehensive
276 analysis,Energies 17(4), 947 (2024).
277 **[10]**Gitelman, L.D. and Kozhevnikov, M.V., New approaches to the concept of energy
278 transition in the times of energy crisis, Sustainability 15(6), 5167 (2023).
279 **[11]**Fridleifsson, I.B., Geothermal energy for the benefit of the people, Renewable and
280 Sustainable Energy Reviews 5(3), 299–312 (2001).
281 **[12]**Fridleifsson, I.B., Status of geothermal energy amongst the world's energy sources,
282 Geothermics, 32(4–6), 379–388 (2003).
283 **[13]**Avtar, R., Sahu, N., Aggarwal, A.K., Chakraborty, S., Kharrazi, A., Yunus, A.P., Dou, J.,
284 and Kurniawan, T.A., Exploring renewable energy resources using remote sensing and
285 GIS—A review, Resources 8(3), 149 (2019).

[14]Gorman, W., Kemp, J.M., Rand, J., Seel, J., Wiser, R., Manderlink, N., Kahrl, F., Porter, K., and Cotton, W., Grid connection barriers to renewable energy deployment in the United States, Joule 9(2) (2025).

[15]Bogdanov, D., Ram, M., Khalili, S., Aghahosseini, A., Fasihi, M., and Breyer, C., Effects of direct and indirect electrification on transport energy demand during the energy transition, Energy Policy 192, p. 114205 (2024).

[16]Aghahosseini, A., Bogdanov, D., Barbosa, L.S., and Breyer, C., Analyzing the feasibility of powering the Americas with renewable energy and interregional grid interconnections by 2030, Renewable and Sustainable Energy Reviews 105, 187–205 (2019).

[17]Carrasco, J.M., Franquelo, L.G., Bialasiewicz, J.T., Galván, E., Portillo-Guisado, R.C., Prats, M.M., León, J.I., and Moreno-Alfonso, N., Power-electronic systems for the grid integration of renewable energy sources: A survey, IEEE Transactions on Industrial Electronics 53(4), 1002–1016 (2006).

[18]M. Singh, V. Khadkikar, A. Chandra, and R. K. Varma, "Grid interconnection of renewable energy sources at the distribution level with power-quality improvement features," IEEE Transactions on Power Delivery 26, 307–315 (2011).

[19]Akagi, H., Active Harmonic Filters, Proceedings of the IEEE 93, 2128–2141 (2005).

[20]Y. Bouzelata, E. Kurt, R. Chenni, and N. Altm, Design and simulation of a unified power quality conditioner fed by solar energy, International Journal of Hydrogen Energy, 40, 15267–15277 (2015).

[21]Das, S.R., Ray, P.K., Sahoo, A.K., Ramasubbareddy, S., Babu, T.S., Kumar, N.M., Elavarasan, R.M., and Mihet-Popa, L., A comprehensive survey on different control strategiesand applications of active power filters for power quality improvement, Energies 14(15), 4589 (2021).

[22]Ali, Z.M., Ćalasan, M., Jurado, F., and Aleem, S.H.A., Complexities of power quality and harmonic-induced overheating in modern power grids: Challenges and solutions, IEEE Access, 12, pp. 151554–151597 (2024).